Kelsey L. Kleinhans
Orthopaedic Biomechanics Laboratory,
Department of Biomedical Engineering,
University of Miami,
1251 Memorial Drive, MEA 219,
Coral Gables, FL 33146
e-mail: k.kleinhans@umiami.edu

Lukas M. Jaworski
Orthopaedic Biomechanics Laboratory,
Department of Biomedical Engineering,
University of Miami,
1251 Memorial Drive, MEA 219,
Coral Gables, FL 33146
e-mail: l.jaworski@umiami.edu

Michaela M. Schneiderbauer
Department of Orthopaedics,
University of Miami Miller School of Medicine,
1400 NW 12th Avenue, Room 4056,
Miami, FL 33136
e-mail: MSchneiderbauer@med.miami.edu

Alicia R. Jackson[1]
Orthopaedic Biomechanics Laboratory,
Department of Biomedical Engineering,
University of Miami,
1251 Memorial Drive, MEA 219,
Coral Gables, FL 33146
e-mail: a.jackson2@miami.edu

Effect of Static Compressive Strain, Anisotropy, and Tissue Region on the Diffusion of Glucose in Meniscus Fibrocartilage

Osteoarthritis (OA) is a significant socio-economic concern, affecting millions of individuals each year. Degeneration of the meniscus of the knee is often associated with OA, yet the relationship between the two is not well understood. As a nearly avascular tissue, the meniscus must rely on diffusive transport for nutritional supply to cells. Therefore, quantifying structure–function relations for transport properties in meniscus fibrocartilage is an important task. The purpose of the present study was to determine how mechanical loading, tissue anisotropy, and tissue region affect glucose diffusion in meniscus fibrocartilage. A one-dimensional (1D) diffusion experiment was used to measure the diffusion coefficient of glucose in porcine meniscus tissues. Results show that glucose diffusion is strain-dependent, decreasing significantly with increased levels of compression. It was also determined that glucose diffusion in meniscus tissues is anisotropic, with the diffusion coefficient in the circumferential direction being significantly higher than that in the axial direction. Finally, the effect of tissue region was not statistically significant, comparing axial diffusion in the central and horn regions of the tissue. This study is important for better understanding the transport and nutrition-related mechanisms of meniscal degeneration and related OA in the knee. [DOI: 10.1115/1.4031118]

Introduction

The degeneration of the meniscus has been consistently connected with the occurrence of OA in the knee, although the mechanisms linking the two remain unclear. The knee meniscus is a fibrocartilaginous tissue that performs an essential role in the knee joint, distributing the majority of the load and maintaining congruency and lubrication [1]. Although it is known that degeneration is a common problem in the knee meniscus, the pathophysiology behind it has not been investigated completely. Much research has been done regarding the meniscal structure, meniscal tears, regeneration, and the biomechanical and anatomical forces endured by the meniscus, but more is needed in order to fully understand the role that menisci play in the function and pathology of the human knee [1–3].

The lack of full vascularization is a distinctive property of knee meniscal tissues. During prenatal development until shortly after birth, the meniscus is fully vascularized [1]. Over time, however, the majority of vascularization appears to subside [1]. Due to incomplete vascularization, the knee meniscus relies on the transport of fluid and solutes through the extracellular matrix (ECM) for providing the necessary nutrients to cells [1]. Transport may occur by diffusive processes or by fluid flow (i.e., convection) through the ECM and is highly dependent upon tissue structure and composition as well as tissue loading conditions. It is believed that the main mechanism of transport for small solutes in avascular cartilaginous tissues is diffusion [4–6]. To understand the transport mechanisms and pathways in knee meniscus, determining the diffusion coefficient (i.e., diffusivity, a measure of solute mobility) for small solutes (e.g., glucose) is important.

Numerous investigators have examined the mechanical properties in meniscus fibrocartilage from human and animal sources. Several studies have found that the meniscus exhibits anisotropic mechanical behavior in tension, compression, and shear loading conditions [7–16]. Furthermore, the mechanical properties of meniscus tissues have been found to be strain-dependent [13,17–20]. However, few studies have investigated transport properties in knee meniscus tissues. Danzig et al. found that continuous passive motion does not significantly affect meniscal nutrition, indicating that diffusion is an important mechanism for transport of nutrients in the tissue [21]. Most recently, Travascio et al. measured the diffusion coefficient of fluorescein in meniscus fibrocartilage using fluorescence recovery after photobleaching and found an anisotropic trend [22]. No previous study has reported on the anisotropic, strain-dependent, or inhomogeneous behavior of nutrient (i.e., glucose) diffusion in the knee meniscus. Such information is necessary to better elucidate the nutritional environment in meniscus tissue and thus more clearly understand tissue pathology.

In the present study, a 1D steady-state diffusion experiment was used to determine the value of the apparent glucose diffusion coefficient in porcine knee meniscus. Similar methods have been employed to determine solute diffusion coefficients in cartilage and intervertebral disk tissues [23–27]. It was hypothesized that the diffusion of glucose in porcine knee meniscus tissue is strain-dependent due to changes in the water content caused by compression. It was also hypothesized that glucose diffusion coefficient in the meniscus is anisotropic, due to the structure of the tissue. Finally, we hypothesized that the diffusion of glucose in meniscus tissue does not vary with regional location (i.e., horn versus central regions), based on previous studies investigating the inhomogeneous behavior of hydraulic permeability in the meniscus [8,10]. Therefore, the objective of this study was to test these hypotheses by measuring the apparent glucose diffusion coefficient of porcine knee meniscus in two directions (axial and

[1]Corresponding author.
Manuscript received February 25, 2015; final manuscript received July 14, 2015; published online August 10, 2015. Assoc. Editor: James C. Iatridis.

circumferential), from two locations (horn and central), and under three levels of static compressive strain (0%, 10%, and 20%).

Materials and Methods

Specimen Preparation. Lateral and medial menisci were harvested from both left and right cadaveric knees of Yorkshire pigs (99.7 ± 6.1 kg, range: 89.4–108.0 kg, ~20–25 weeks, both male and females) obtained from a local slaughterhouse within 1 hr of death. A total of 14 menisci were harvested from eight pigs. Cylindrical specimens (6 mm diameter and ~0.5 mm thickness) were prepared using a stainless steel corneal trephine (Biomedical Research Instruments, Inc., Malden, MA) and sledge microtome (Model SM2400, Leica Instruments, Nussloch, Germany) with freezing stage (Model BFS-30, Physitemp Instruments, Inc., Clifton, NJ). The height was measured using a custom current-sensing micrometer that works using a capacitive sensor to read the height of the tissue sample and is precise to 0.001 mm. Samples were excised in the axial and circumferential directions, see Fig. 1. Samples from both medial and lateral menisci from both left and right knees were pooled. In the axial direction, samples were taken from both the horn and the central regions, as shown in Fig. 1, while circumferential samples were only taken from the central region. A total of three groups of specimens were tested: axial horn (A-H) ($n = 10$), axial central (A-C) ($n = 10$), and circumferential central (C-C) ($n = 10$). Three tests, corresponding to three levels of compressive strain (0%, 10%, and 20%), were performed on each sample specimen. In this study, the samples were compressed 10% and 20%, as these strain levels have been previously studied and are known to be in the range of physiological meniscal strains occurring in daily activity [13,28–32].

Tissue Water Volume Fraction Measurement. Each sample was cut from a core of tissue (see Fig. 1) and the adjacent tissue from the core was saved and frozen at −20 °C to perform water volume fraction measurements. The volume fraction of water for each core was calculated by a buoyancy method, Eq. (1), published in literature [33,34]. The weight of the core specimen in air, W_{wet}, and the weight in phosphate-buffered saline (PBS), W_{PBS}, were measured using a density determination kit of an analytical balance (Model ML104, Mettler Toledo, Columbus, OH). Following lyophilization, the weight of the dry core specimen, W_{dry}, was measured. The volume fraction of water, ϕ^w, of the core specimens was calculated by

$$\phi^w = \frac{W_{wet} - W_{dry}}{W_{wet} - W_{PBS}} \frac{\rho_{PBS}}{\rho_{H_2O}} \tag{1}$$

where ρ_{PBS} and ρ_{H_2O} are the mass densities of PBS and water, respectively.

Following the water volume fraction calculation, the strain-dependent water volume fraction can be estimated at each compressive strain level (0%, 10%, and 20%) using the relationship

$$\phi^w = \frac{\phi_o^w + e}{1 + e} \tag{2}$$

where ϕ_o^w is the water volume fraction of the undeformed tissue calculated from Eq. (1), and the relative volume change is related to deformation by $e(=J-1)$, where J is the ratio of the current tissue volume to the undeformed tissue volume [23,35].

Diffusion Coefficient Measurement. A custom-made diffusion apparatus was constructed as shown in Fig. 2 to measure the strain-dependent diffusion coefficient of glucose in meniscus tissue based on previous studies [23–25]. The device consists of two cylindrical acrylic solution chambers divided by a specimen holder in the middle. The volume of the larger, upstream chamber is 1000 μL, while that of the smaller, downstream chamber is 200 μL. The diameters of the chambers allowed for the volumes to have similar heights of solution, thus negating gravitational force as an additional driving force for transport across the tissue specimen.

The specimen is held between two semi-rigid polyethylene porous plates (hydrophilic polyethylene, 50–90 μm pore size, Small Parts, Inc., Miami Lakes, FL) (diameter = 5 mm) with 50% open area and sealed radially with an o-ring (Buna-N metric rubber, Small parts, Inc., Miami Lakes, FL) (inner diameter = 6 mm and thickness = 2 mm). The 50% open area and 5 mm diameter of the porous plates were used to determine the area of diffusive flux across the tissue, in order to calculate the diffusion coefficient using Eq. (3). The level of compressive strain (0%, 10%, and 20%) is controlled by adjusting the size of the spacer between the chamber halves to within 0.01 mm of the tissue size. Stirring bars (VWR International, Suwannee, GA) ensure that the solutions in the upstream and downstream chambers are continuously moving to allow homogeneous concentration and reduce boundary layer formation.

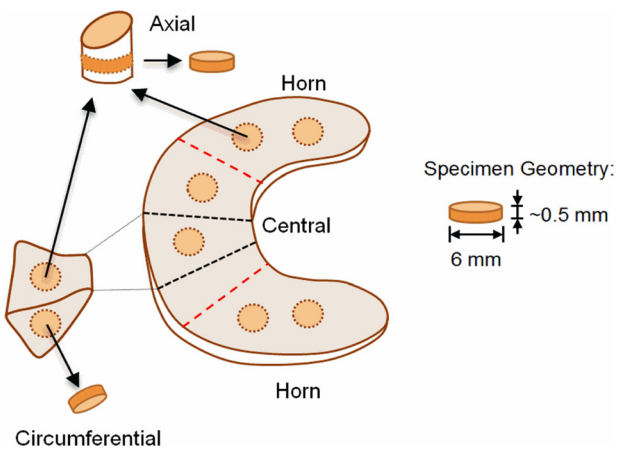

Fig. 1 Schematic showing locations and sizes of test specimens. The meniscus was divided into central and horn regions (demarcated by larger dashed lines). From the central region, both axial and circumferential specimens were prepared; only axial specimens were prepared from the horn region. All specimens were cylindrical with a height of ~0.5 mm and a diameter of 6 mm. Note that axial specimens were taken from the central region of the core of tissue. Samples from both medial and lateral menisci were pooled.

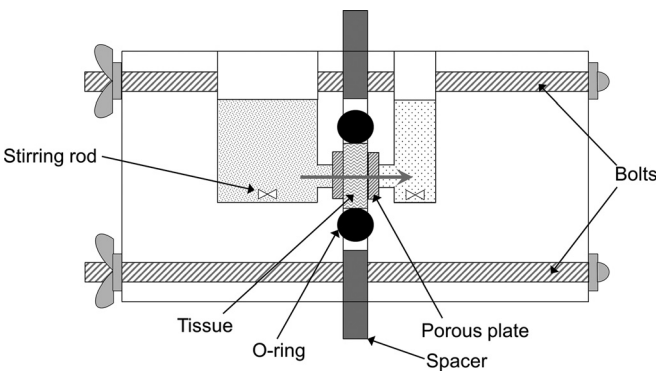

Fig. 2 Schematic of the custom-designed chamber for measuring the diffusion coefficient. The metal spacers between the two chamber halves are used to control the amount of uniaxial confined compression on the specimen; that is, the spacer matches the desired compressed height of the tissue (i.e., for a 0.5 mm thick specimen at 0% strain, the spacer is 0.5 mm, while at 10% strain the spacer is changed to 0.45 mm thickness).

A 1D steady-state diffusion experiment was employed to measure the glucose diffusion coefficient in meniscus as seen in previous studies [23–27]. The specimen was placed in the sealed chamber and allowed to equilibrate for approximately 20 min. At the start of the experiment, high glucose PBS solution (20 g/L, Sigma-Aldrich Co., St. Louis, MO) was added to the upstream chamber, while blank PBS solution was loaded in the downstream chamber. At 15 min time intervals, all 200 μL of the downstream chamber solution was removed and a fresh 200 μL of blank PBS solution was added. A sample (1 μL) of the extracted 200 μL solution was then used to measure the glucose levels in the downstream chamber using a custom-modified diabetic glucose meter (Accu-Chek Aviva, Roche Diagnostics, Indianapolis, IN) in concert with a sourcemeter (Keithley SourceMeter, Cleveland, OH) and custom LABVIEW (National Instruments, Austin, TX) software. A standard calibration curve was used to determine the glucose concentration measurements from recorded current readings; for all experiments, the calibration curve had an $R^2 \geq 0.98$.

Once steady state (2–3 consecutive measurements within the same (~5%) concentration) was achieved for specimens at 0% compression, the experiment was repeated for 10% and 20% compressive strains. When the downstream concentration reached steady state, the apparent diffusion coefficient, D_{app} ($= \phi D$, where ϕ is the partition coefficient, and D is the effective diffusion coefficient), was calculated from [23–25,36]

$$D_{app} = \ln\left(\frac{C_{up}}{C_{up} - C_{down}(t)}\right)\frac{V_{down}h}{A(t)} \tag{3}$$

where C_{up} is the solute concentration in the upstream chamber (the high-concentration side), C_{down} is the solute concentration in the downstream chamber, V_{down} is the volume in the downstream chamber, t is the time interval (in this case, 15 min), and A and h are the diffusion area and diffusion distance (equal to specimen thickness after compression), respectively. Tests were carried out at room temperature (~23 °C).

Scanning Electron Microscopy. Scanning electron microscopy (SEM) images of porcine meniscal tissues were obtained in order to compare the collagen fiber structure to the diffusion coefficient results. Axial and circumferential slices of knee meniscus tissues from the central region, prepared as described above, were fixed with a 2% glutaraldehyde (Sigma-Aldrich Co., St. Louis, MO) in PBS solution (Sigma-Aldrich Co., St. Louis, MO). Samples were then dehydrated in a graded series of ethanol (20%, 50%, 70%, 90%, and 100%) and dried by immersion in hexamethyldisilazane (Sigma-Aldrich Co., St. Louis, MO) [37]. The samples were sputter-coated with gold/palladium (Cressington Scientific 108auto Sputter Coater, Redding, CA). High-resolution SEM images were obtained using an Environmental Scanning Electron Microscope (FEI/Phillips XL-30 FEG ESEM, Hillsboro, OR).

Statistical Analysis. A total of ten specimens were tested for each of the nine groups (=3 location/direction groups × 3 strain levels). Three independent variables were studied: level of compression, direction of diffusion, and regional location. Statistical significance between groups was determined by two 3 × 2 two-way mixed analysis of variance (ANOVA) tests using IBM SPSS STATISTICS 22 (International Business Machines Corp., Armonk, NY). One test was performed to compare axial central and axial horn groups, to determine if significant regional variation was present, while another compared axial central and circumferential central, to determine if significant anisotropy was present. The significance level was set at $p < 0.025$ (based on the Bonferroni Correction). For both ANOVA tests, effect of compression was investigated using repeated measures. Least significant difference (LSD) post-hoc analysis with the Bonferroni correction was performed using SPSS software to determine between which groups there was a significant difference. All data are given in mean ± standard deviation.

One-way ANOVA was performed to determine if water volume fraction and height measurements differed significantly between the three test groups (A-C, A-H, and C-C). Regression analysis was performed to determine if the relationships between relative diffusion coefficient and water volume fraction, and diffusion coefficient and strain level were statistically significant.

Results

The results for the glucose diffusion coefficient for the three groups investigated are shown in Table 1; data are shown as mean ± standard deviation. Results show that the diffusion coefficient decreases with increasing level of compressive strain for all groups investigated. On average, 10% compression led to a ~30% decrease in the diffusion coefficient compared to values in uncompressed tissues; 20% compression led to an additional ~26% decrease in the diffusion coefficient (compared to values at 10% compression). We also found that glucose diffusion in the circumferential direction was greater than that in the axial direction in the central region; the ratio of C-C to A-C was 1.39 at 0% compression, 1.51 at 10% compression, and 1.42 at 20% compression. Two-way mixed ANOVA indicated that the glucose diffusion coefficient was significantly affected by both compression ($p < 0.001$) and direction of diffusion ($p < 0.025$) when comparing the axial central and circumferential central groups. However, two-way mixed ANOVA showed that the diffusion coefficient was not significantly affected by region in the tissue when comparing axial central and axial horn groups ($p = 0.281$), although a significant effect of compression was still seen ($p < 0.001$). LSD post-hoc analysis with the Bonferroni correction indicated that the diffusion coefficient in the circumferential direction was significantly ($p < 0.025$) higher than that in the axial direction at all three levels of compression. Post-hoc analysis also showed that, for each of the three groups investigated, when comparing the diffusion coefficient at 0% and 10% compression and at 10% and 20% compression, results were significantly ($p < 0.025$) different.

Figure 3 shows regression analysis for the relationship between apparent diffusion coefficient and level of compressive strain. For all three groups, there was a significant correlation detected between diffusion and strain level, as noted by the p values, see Fig. 3. This further illustrates the significant effects of compression on transport in meniscus fibrocartilage.

The averaged water volume fraction values of the three groups at three levels of compressive strain are shown in Table 1; there were no significant differences between groups. The mean height of the three groups under zero compression conditions was 0.58 ± 0.06 mm for A-H, 0.54 ± 0.08 mm for A-C, and 0.54 ± 0.08 mm for C-C; again, there were no significant differences between groups. The relative diffusion coefficient, D_{app}/D_o

Table 1 Results for water volume fraction (ϕ^w), apparent diffusion coefficient (D_{app}), and relative diffusion coefficient (D_{app}/D_o) for the groups investigated: (a) axial horn (A-H), (b) axial central (A-C), and (c) circumferential central (C-C). All values are shown in mean ± standard deviation.

	Strain (%)	N	ϕ^w	D_{app} ($\times 10^{-6}$ cm^2/s)	D_{app}/D_o
A-H	0	10	0.71 ± 0.03	1.81 ± 0.76	0.28 ± 0.12
	10	10	0.68 ± 0.04	1.33 ± 0.44	0.21 ± 0.07
	20	10	0.64 ± 0.04	1.11 ± 0.51	0.17 ± 0.08
A-C	0	10	0.73 ± 0.05	1.68 ± 0.69	0.26 ± 0.11
	10	10	0.70 ± 0.06	1.10 ± 0.39	0.17 ± 0.06
	20	10	0.66 ± 0.07	0.79 ± 0.14	0.12 ± 0.02
C-C	0	10	0.70 ± 0.02	2.33 ± 1.27	0.36 ± 0.20
	10	10	0.67 ± 0.03	1.66 ± 0.71	0.26 ± 0.11
	20	10	0.63 ± 0.03	1.12 ± 0.42	0.18 ± 0.07

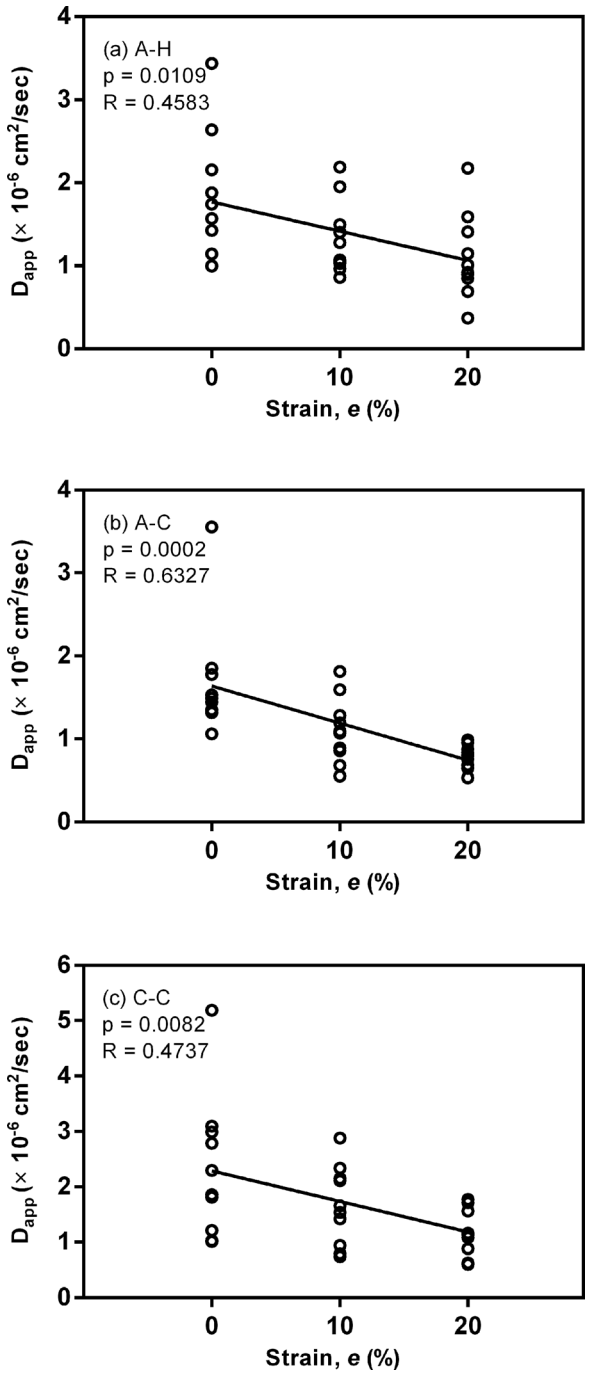

Fig. 3 Correlation between apparent glucose diffusion coefficient and level of compression for three groups investigated: (*a*) axial horn (A-H), (*b*) axial central (A-C), and (*c*) circumferential central (C-C). Significant correlation was detected for all groups; *p* values and *R* values are shown for each.

(where D_o is the diffusion coefficient of glucose in aqueous solution ($D_o = 6.38 \times 10^{-6}$ cm^2/s)) [38], of glucose in porcine meniscus at three levels of compression is also shown in Table 1. Statistical significance for relative diffusion data is the same as that for apparent diffusion coefficient discussed above, given that relative diffusion is simply a scaled value.

Given the significant anisotropic findings for the glucose diffusion coefficient determined here (i.e., circumferential diffusivity > axial diffusivity), SEM images were acquired to investigate the relationship between tissue morphology and anisotropic transport; images are shown in Fig. 4. SEM images show the collagen fibers aligned perpendicular to the axial direction, as shown in Figs. 4(*a*) and 4(*c*), thereby creating porous channels in the circumferential direction; one such channel is circled in the figure. Note that channels are not present in the axial direction, see Figs. 4(*b*) and 4(*d*).

In addition, we have included scatter plots showing the relationship between tissue water volume fraction, ϕ^w, and relative diffusion, $D_{app}/D_{o,}$ for each of the three groups tested: A-H samples ($n = 30$) (Fig. 5(*a*)); A-C samples ($n = 30$) (Fig. 5(*b*)); and C-C samples ($n = 30$) (Fig. 5(*c*)). Regression analysis revealed a significant ($p < 0.001$) relationship for all three groups investigated when the best fit line is assumed to pass through the origin (0,0). The values for tissue water volume fraction for compressed samples were calculated based on Eq. (2) at strain levels of 10% ($e = -0.1$) and 20% ($e = -0.2$).

Discussion

In this study, we investigated the effects of compression, anisotropy, and tissue region on the apparent diffusion coefficient of glucose in meniscal fibrocartilage using a 1D diffusion experiment. To the best of our knowledge, this is the first study to quantify glucose diffusion in meniscus tissues. The values determined here are similar to those in the literature for glucose diffusion coefficients in other cartilaginous tissues (e.g., articular cartilage and intervertebral disk), which ranged from 0.138 to 6.08×10^{-6} cm^2/s [23,24,26,39–45]. Furthermore, the value for relative diffusion of glucose in meniscus fibrocartilage (average of 0.30 ± 0.15 for all groups at 0% compression) is similar to results in the literature, which indicate that it is in the range of 0.3–0.38 for articular cartilage (under zero compression conditions) [42,44].

Effect of Compression. The experimental results of this study show that the apparent glucose diffusion coefficient in porcine knee meniscus tissues is significantly affected by the level of compressive strain applied. The decrease in diffusion as the level of compression increases is likely due to the changes in tissue water content caused by the application of compressive strain. According to Eq. (2), with each additional 10% compression, the water volume fraction of the tissue decreases by ~3% to 4%. The diffusion of solutes in cartilaginous tissues is highly dependent upon tissue water content, generally showing a positive correlation [22,23,46–53]. Indeed, several models for solute diffusion in hydrated porous media, such as meniscus fibrocartilage, show that the diffusion coefficient is directly related to tissue water volume fraction [51,54]. The relationship between water volume fraction and relative diffusion coefficient is shown in Fig. 5. Regression analysis showed a significant relationship between water volume fraction and apparent diffusion coefficient for all groups studied.

The strain-dependent behavior of glucose diffusion coefficient found here is similar to results in the literature for diffusion of solutes in other cartilaginous tissues under compression. Numerous investigators have found that static loading results in reduced diffusion of solutes of various sizes in articular cartilage [29,30,39,50,55–57]. Furthermore, previous work has shown that the diffusion of glucose is strain-dependent in intervertebral disk tissues [23,24].

Effect of Anisotropy. Our results also indicate that diffusion of glucose in meniscus tissues is anisotropic (i.e., direction-dependent). It was found that the apparent glucose diffusion coefficient in the central region in the axial direction was significantly less than that in the circumferential direction at all levels of compressive strain. Travascio et al. previously found that the diffusion of fluorescein (MW = 332 Da) in meniscus tissues is anisotropic, with an anisotropic ratio of 3 in the tissue [22]. In the present study, we have found that the diffusion coefficient in the circumferential direction was ~1.4× that in the axial direction under zero strain conditions. Similar anisotropic results have been found for

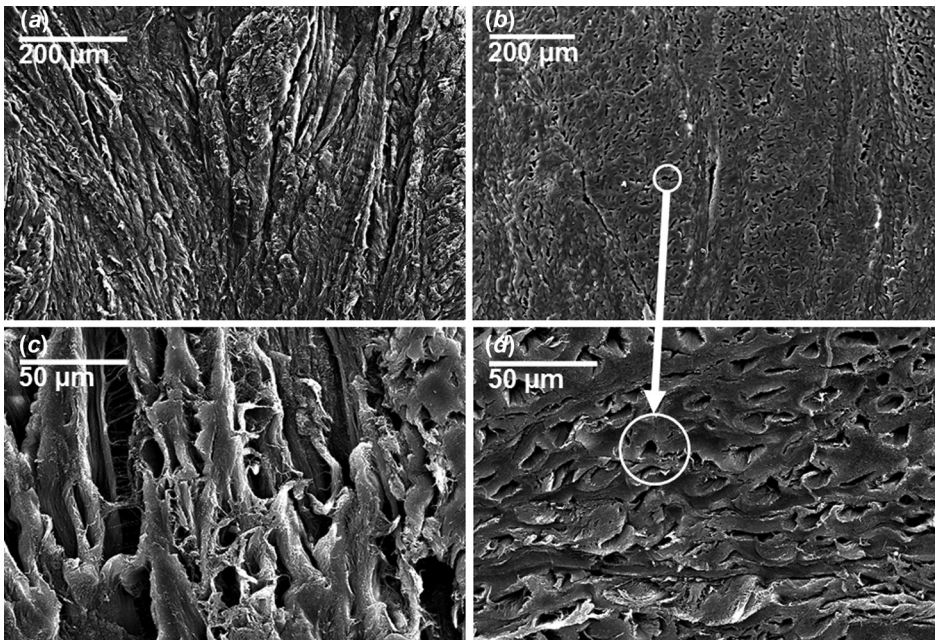

Fig. 4 SEM images of both axial ((*a*) and (*c*)) and circumferential ((*b*) and (*d*)) porcine meniscus samples. Images (*a*) and (*b*) are magnified 250× with scale bars equaling 200 μm, while (*c*) and (*d*) are magnified 1000× with scale bars equaling 50 μm. Note the collagen fiber bundles running in the circumferential direction, thereby allowing for the presence of pores in circumferential specimens that are not apparent in axial specimens. The circle on (*b*) shows an example of a channel in the circumferential direction with the arrow pointing to (*d*) showing a magnified version of a channel. The samples were fixed using a 2% glutaraldehyde in PBS solution, dehydrated in a graded series of ethanol (20%, 50%, 70%, 90%, and 100%), and dried by immersion in hexamethyldisilazane.

solute diffusion in cartilaginous tissues [23,24,46,49,53,58–62]. It should be noted that there were no significant differences in the tissue water volume fraction values for axial and circumferential specimens (values shown in Table 1), indicating that the difference in the diffusion coefficient found for the two directions is not likely to be attributed to variations in tissue composition alone.

In order to fully understand the anisotropic results found here, SEM images of axial (Figs. 4(*a*) and 4(*c*)) and circumferential (Figs. 4(*b*) and 4(*d*)) meniscus samples from the central region were obtained. The SEM images show the collagen fibers aligned perpendicular to the axial direction, and thus parallel to the circumferential direction (i.e., collagen fiber bundles are oriented in the circumferential direction). As seen in Fig. 4(*b*), the alignment of the collagen fibers in the circumferential direction allows for the presence of pores that are not apparent in the axial direction; see notation in Figs. 4(*b*) and 4(*d*). This pore structure may allow glucose to move more freely in the circumferential direction, parallel to the collagen fiber bundles. Indeed, previous studies have found the diffusion coefficient to be significantly higher in the direction parallel to collagen fibers (i.e., circumferential) in cartilaginous tissues [58,63]. Furthermore, similar pore structure has also been found in other cartilaginous tissues, termed either microtubules or tubules [46,64–66]. This is in agreement with our data showing that the particular organization of collagen fibers contributes to the anisotropic transport behavior of glucose in meniscus fibrocartilage. It should be noted that this organization of collagen fibers has been previously established for the deep (interior) layer of the meniscus [7,67]; samples for diffusion experiments and imaging studies were both harvested from this deep layer.

Effect of Tissue Region. Additionally, our results indicate that there is no statistically significant variation in the apparent diffusion coefficient when comparing axial diffusion in different tissue regions (i.e., horn versus central regions). This is in agreement with our hypothesis that the glucose diffusion coefficient would not vary with location of the tissue specimen (central versus horn regions). These findings are consistent with results in the literature showing that fluid transport (i.e., hydraulic permeability) in meniscus tissues is homogeneous [8,10]. The lack of statistical significance found in this study may be attributed to several factors. First, only ten samples ($n = 10$) were tested for each of the groups and thus sample size was small. Furthermore, regional variation was only investigated for axially oriented tissue specimens; however, given the anisotropic results found here and the dependence on the particular structure of the tissue, the diffusion coefficient in other directions (e.g., circumferential) may be affected by tissue region and deserves further study.

Limitations. There are several limitations to this study that should be noted. Although the use of human tissues to calculate the apparent diffusion coefficient is preferred, we studied diffusion in porcine meniscus tissues due to easy availability of porcine knee joints. Moreover, it has been found that porcine meniscus tissues have similar properties to human meniscus tissues [3,10,68]. A study by Chu et al. found porcine specimens to be good models for human cartilage studies, showing similarities in joint size, structure, and cartilage thickness [69]. Therefore, our results using porcine tissues are expected to be indicative of trends in human meniscus, if not exact quantities. In the future, human tissues will be investigated.

An additional limitation in this study was the use of the porous plates in the custom-made diffusion chamber. While we do not anticipate a large change in the results due to the use of these plates, it is possible that there was a stagnant layer formed on the boundary of the porous plates, thus influencing our results. This build-up was minimized by the use of stirring rods and continuous movement of the fluid throughout the experiment. These porous

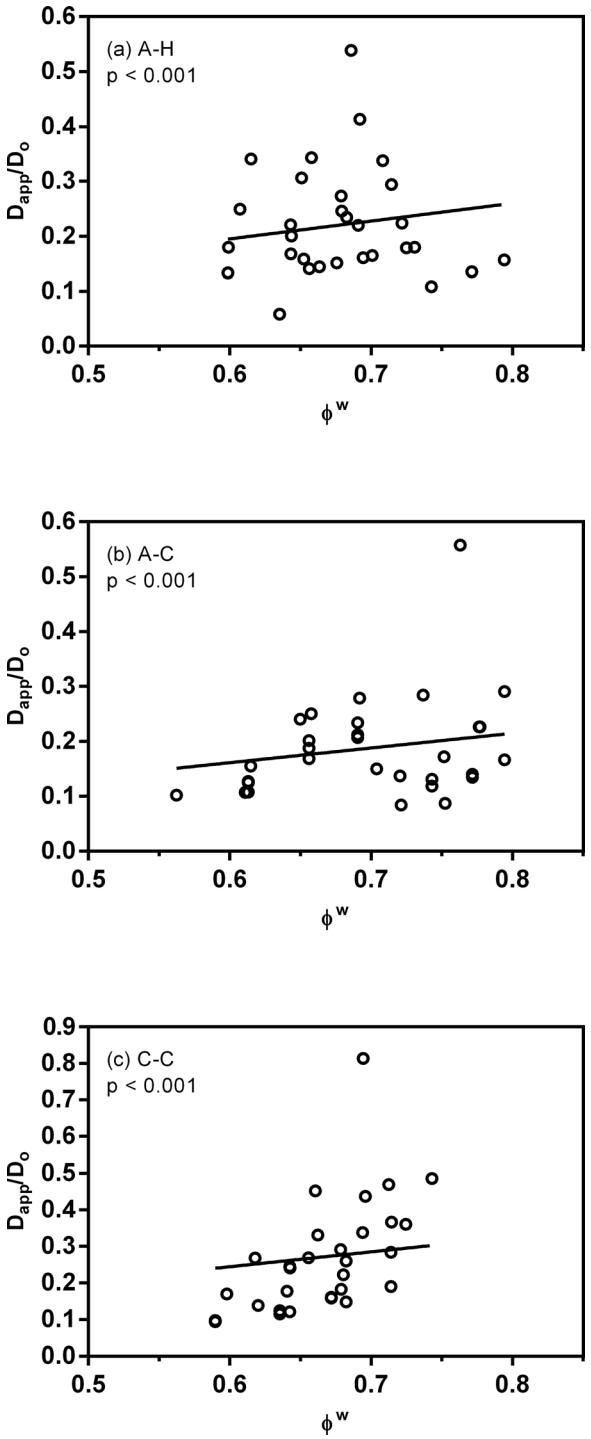

Fig. 5 Relationship between tissue water volume fraction, ϕ^w, and relative diffusion coefficient, D_{app}/D_o, in meniscus tissues for the three groups investigated: (*a*) axial, horn; (*b*) axial, central; and (*c*) circumferential, central. For all groups, $n = 30$. *P* values from regression analysis assuming no constant (i.e., best fit line passing through the origin) are shown for each group.

plates were necessary to hold the tissue in place, minimize swelling, and allow for compression. Previous studies by Jackson et al. showed a reduction in the diffusion coefficient by 7% with the use of porous plates [23]; this was most likely due to the build-up of a stagnant layer at the tissue boundary.

Finally, in this study we used samples from both medial and lateral menisci, but in only axial and circumferential directions. In the future, we will be studying all three principal directions (i.e., axial, radial, and circumferential) while further investigating regional variations (central versus horn locations) and comparing medial to lateral meniscus, given that there are mixed findings in previous studies as to the inhomogeneity of mechanical properties of meniscus tissues [7,8,10,17,19]. Additionally, while samples in this study all came from similarly aged pigs and were considered healthy tissue, further studies are necessary in order to understand the effects of tissue degeneration on transport behavior in meniscus fibrocartilage. These future studies will provide a full characterization of the nutritional transport environment within the meniscus under numerous physiologically relevant conditions. Nonetheless, the results of this study provide important information regarding nutritional supply in the tissue and serve as a launching point for this proposed work.

Conclusion

In summary, this study investigated the strain-dependent, anisotropic, and region-dependent diffusion of glucose in porcine meniscus fibrocartilage. It was found that the apparent glucose diffusion coefficient is significantly affected by mechanical compression, which decreases as strain is increased. It was also found that diffusion of glucose in the circumferential direction, along the primary direction of the collagen fibers, is significantly higher than in the axial direction. Finally, there was no statistically significant difference in axial glucose diffusion comparing the central and horn regions of the meniscus. Given the importance of a healthy meniscus in the proper functioning of the knee joint, as well as the unknown role of the tissue in the onset and progression of OA, better understanding of the transport environment within the tissue and the relationship with tissue pathophysiology is essential in the development of new strategies to treat and/or prevent tissue degeneration and related OA. This study provides baseline information on the structure–function relationships for solute transport properties in the meniscus and establishes the methods necessary to move toward full characterization of nutritional transport in meniscus fibrocartilage.

Acknowledgment

The authors would like to thank Dr. Pat Blackwelder for assistance with SEM imaging and Adam Bofill for assistance in apparatus development. This project was funded by the University of Miami College of Engineering.

Nomenclature

A = area of diffusion
A-C = axial, central
A-H = axial, horn
ANOVA = analysis of variance
C_{down} = concentration in the downstream chamber
C_{up} = concentration in the upstream chamber
C-C = circumferential, central
D_{app} = apparent diffusion coefficient
D_o = diffusion coefficient in aqueous solution
e = deformation
ECM = extracellular matrix
FRAP = fluorescence recovery after photobleaching
h = height of tissue, equal to the tissue thickness
J = relative volume change
LSD = least significant difference
OA = osteoarthritis
PBS = phosphate-buffered saline
SEM = scanning electron microscopy
t = time
V_{down} = volume of solution in the downstream chamber
W_{dry} = weight of dry tissue specimen (following lyophilization)

W_{PBS} = weight of tissue specimen in phosphate-buffered saline solution
W_{wet} = weight of tissue specimen in air
1D = one-dimensional
ρ_{H_2O} = density of water
ρ_{PBS} = density of phosphate-buffered saline solution
ϕ^w = tissue water volume fraction
ϕ_o^w = water volume fraction of uncompressed tissue
Φ = partition coefficient

References

[1] Makris, E. A., Hadidi, P., and Athanasiou, K. A., 2011, "The Knee Meniscus: Structure-Function, Pathophysiology, Current Repair Techniques, and Prospects for Regeneration," Biomaterials, **32**(30), pp. 7411–7431.

[2] Andriacchi, T. P., Mundermann, A., Smith, R. L., Alexander, E. J., Dyrby, C. O., and Koo, S., 2004, "A Framework for the In Vivo Pathomechanics of Osteoarthritis at the Knee," Ann. Biomed. Eng., **32**(3), pp. 447–457.

[3] Sweigart, M. A., and Athanasiou, K. A., 2005, "Biomechanical Characteristics of the Normal Medial and Lateral Porcine Knee Menisci," Proc. Inst. Mech. Eng., Part H, **219**(1), pp. 53–62.

[4] Maroudas, A., 1975, "Biophysical Chemistry of Cartilaginous Tissues With Special Reference to Solute and Fluid Transport," Biorheology, **12**(3–4), pp. 233–248.

[5] Urban, J. P., Holm, S., Maroudas, A., and Nachemson, A., 1982, "Nutrition of the Intervertebral Disc: Effect of Fluid Flow on Solute Transport," Clin. Orthop. Relat. Res., **170**, pp. 296–302.

[6] Urban, J. P., Holm, S., and Maroudas, A., 1978, "Diffusion of Small Solutes Into the Intervertebral Disc: An In Vivo Study," Biorheology, **15**(3–4), pp. 203–221.

[7] Fithian, D. C., Kelly, M. A., and Mow, V. C., 1990, "Material Properties and Structure-Function Relationships in the Menisci," Clin. Orthop. Relat. Res., **252**, pp. 19–31.

[8] Proctor, C. S., Schmidt, M. B., Whipple, R. R., Kelly, M. A., and Mow, V. C., 1989, "Material Properties of the Normal Medial Bovine Meniscus," J. Orthop. Res., **7**(6), pp. 771–782.

[9] Nguyen, A. M., and Levenston, M. E., 2012, "Comparison of Osmotic Swelling Influences on Meniscal Fibrocartilage and Articular Cartilage Tissue Mechanics in Compression and Shear," J. Orthop. Res., **30**(1), pp. 95–102.

[10] Sweigart, M. A., Zhu, C. F., Burt, D. M., DeHoll, P. D., Agrawal, C. M., Clanton, T. O., and Athanasiou, K. A., 2004, "Intraspecies and Interspecies Comparison of the Compressive Properties of the Medial Meniscus," Ann. Biomed. Eng., **32**(11), pp. 1569–1579.

[11] Gabrion, A., Aimedieu, P., Laya, Z., Havet, E., Mertl, P., Grebe, R., and Laude, M., 2005, "Relationship Between Ultrastructure and Biomechanical Properties of the Knee Meniscus," Surg. Radiol. Anat., **27**(6), pp. 507–510.

[12] Tissakht, M., and Ahmed, A. M., 1995, "Tensile Stress-Strain Characteristics of the Human Meniscal Material," J. Biomech., **28**(4), pp. 411–422.

[13] Chia, H. N., and Hull, M. L., 2008, "Compressive Moduli of the Human Medial Meniscus in the Axial and Radial Directions at Equilibrium and at a Physiological Strain Rate," J. Orthop. Res., **26**(7), pp. 951–956.

[14] Leslie, B. W., Gardner, D. L., McGeough, J. A., and Moran, R. S., 2000, "Anisotropic Response of the Human Knee Joint Meniscus to Unconfined Compression," Proc. Inst. Mech. Eng., Part H, **214**(6), pp. 631–635.

[15] Skaggs, D. L., Warden, W. H., and Mow, V. C., 1994, "Radial Tie Fibers Influence the Tensile Properties of the Bovine Medial Meniscus," J. Orthop. Res., **12**(2), pp. 176–185.

[16] Spilker, R. L., Donzelli, P. S., and Mow, V. C., 1992, "A Transversely Isotropic Biphasic Finite Element Model of the Meniscus," J. Biomech., **25**(9), pp. 1027–1045.

[17] Sanchez-Adams, J., Willard, V. P., and Athanasiou, K. A., 2011, "Regional Variation in the Mechanical Role of Knee Meniscus Glycosaminoglycans," J. Appl. Physiol., **111**(6), pp. 1590–1596.

[18] Danso, E. K., Honkanen, J. T., Saarakkala, S., and Korhonen, R. K., 2014, "Comparison of Nonlinear Mechanical Properties of Bovine Articular Cartilage and Meniscus," J. Biomech., **47**(1), pp. 200–206.

[19] Bursac, P., Arnoczky, S., and York, A., 2009, "Dynamic Compressive Behavior of Human Meniscus Correlates With Its Extra-Cellular Matrix Composition," Biorheology, **46**(3), pp. 227–237.

[20] LeRoux, M. A., and Setton, L. A., 2002, "Experimental and Biphasic FEM Determinations of the Material Properties and Hydraulic Permeability of the Meniscus in Tension," ASME J. Biomech. Eng., **124**(3), pp. 315–321.

[21] Danzig, L. A., Hargens, A. R., Gershuni, D. H., Skyhar, M. J., Sfakianos, P. N., and Akeson, W. H., 1987, "Increased Transsynovial Transport With Continuous Passive Motion," J. Orthop. Res., **5**(3), pp. 409–413.

[22] Travascio, F., Zhao, W., and Gu, W. Y., 2009, "Characterization of Anisotropic Diffusion Tensor of Solute in Tissue by Video-FRAP Imaging Technique," Ann. Biomed. Eng., **37**(4), pp. 813–823.

[23] Jackson, A. R., Yuan, T. Y., Huang, C. Y., Travascio, F., and Gu, W. Y., 2008, "Effect of Compression and Anisotropy on the Diffusion of Glucose in Annulus Fibrosus," Spine, **33**(1), pp. 1–7.

[24] Jackson, A. R., Yuan, T. Y., Huang, C. Y., Brown, M. D., and Gu, W. Y., 2012, "Nutrient Transport in Human Annulus Fibrosus is Affected by Compressive Strain and Anisotropy," Ann. Biomed. Eng., **40**(12), pp. 2551–2558.

[25] Yuan, T. Y., Jackson, A. R., Huang, C. Y., and Gu, W. Y., 2009, "Strain-Dependent Oxygen Diffusivity in Bovine Annulus Fibrosus," ASME J. Biomech. Eng., **131**(7), p. 074503.

[26] Maroudas, A., Stockwell, R. A., Nachemson, A., and Urban, J., 1975, "Factors Involved in the Nutrition of the Human Lumbar Intervertebral Disc: Cellularity and Diffusion of Glucose In Vitro," J. Anat., **120**(1), pp. 113–130.

[27] Maroudas, A., Bullough, P., Swanson, S. A., and Freeman, M. A., 1968, "The Permeability of Articular Cartilage," J. Bone Jt. Surg., Br. Vol., **50**(1), pp. 166–177.

[28] Martin Seitz, A., Galbusera, F., Krais, C., Ignatius, A., and Durselen, L., 2013, "Stress-Relaxation Response of Human Menisci Under Confined Compression Conditions," J. Mech. Behav. Biomed. Mater., **26**, pp. 68–80.

[29] Quinn, T. M., Kocian, P., and Meister, J. J., 2000, "Static Compression is Associated With Decreased Diffusivity of Dextrans in Cartilage Explants," Arch. Biochem. Biophys., **384**(2), pp. 327–334.

[30] Quinn, T. M., Morel, V., and Meister, J. J., 2001, "Static Compression of Articular Cartilage Can Reduce Solute Diffusivity and Partitioning: Implications for the Chondrocyte Biological Response," J. Biomech., **34**(11), pp. 1463–1469.

[31] Eckstein, F., Lemberger, B., Stammberger, T., Englmeier, K. H., and Reiser, M., 2000, "Patellar Cartilage Deformation In Vivo After Static Versus Dynamic Loading," J. Biomech., **33**(7), pp. 819–825.

[32] Yang, N. H., Canavan, P. K., Nayeb-Hashemi, H., Najafi, B., and Vaziri, A., 2010, "Protocol for Constructing Subject-Specific Biomechanical Models of Knee Joint," Comput. Methods Biomech. Biomed. Eng., **13**(5), pp. 589–603.

[33] Gu, W. Y., Lewis, B., Lai, W. M., Ratcliffe, A., and Mow, V. C., 1996, "A Technique for Measuring Volume and True Density of the Solid Matrix of Cartilaginous Tissues," ASME Adv. Bioeng., **33**, pp. 89–90.

[34] Gu, W. Y., Lewis, B., Saed-Nejad, F., Lai, W. M., and Ratcliffe, A., 1997, "Hydration and True Density of Normal and PG-Depleted Bovine Articular Cartilage," Trans. Orthop. Res. Soc., **22**(2), p. 826.

[35] Lai, W. M., Hou, J. S., and Mow, V. C., 1991, "A Triphasic Theory for the Swelling and Deformation Behaviors of Articular Cartilage," ASME J. Biomech. Eng., **113**(3), pp. 245–258.

[36] Malda, J., Rouwkema, J., Martens, D. E., Le Comte, E. P., Kooy, F. K., Tramper, J., van Blitterswijk, C. A., and Riesle, J., 2004, "Oxygen Gradients in Tissue-Engineered PEGT/PBT Cartilaginous Constructs: Measurement and Modeling," Biotechnol. Bioeng., **86**(1), pp. 9–18.

[37] Hayat, M. A., 1982, *Fixation for Electron Microscope*, Academic Press, New York.

[38] Longsworth, L. G., 1953, "Diffusion Measurements, at 25 °C, of Aqueous Solutions of Amino Acids, Peptides, and Sugars," J. Am. Chem. Soc., **75**(22), pp. 5705–5709.

[39] Burstein, D., Gray, M. L., Hartman, A. L., Gipe, R., and Foy, B. D., 1993, "Diffusion of Small Solutes in Cartilage as Measured by Nuclear Magnetic Resonance (NMR) Spectroscopy and Imaging," J. Orthop. Res., **11**(4), pp. 465–478.

[40] Allhands, R. V., Torzilli, P. A., and Kallfelz, F. A., 1984, "Measurement of Diffusion of Uncharged Molecules in Articular Cartilage," Cornell Vet., **74**(2), pp. 111–123.

[41] Torzilli, P. A., Grande, D. A., and Arduino, J. M., 1998, "Diffusive Properties of Immature Articular Cartilage," J. Biomed. Mater. Res., **40**(1), pp. 132–138.

[42] Maroudas, A., 1968, "Physicochemical Properties of Cartilage in the Light of Ion Exchange Theory," Biophys. J., **8**(5), pp. 575–595.

[43] Torzilli, P. A., Arduino, J. M., Gregory, J. D., and Bansal, M., 1997, "Effect of Proteoglycan Removal on Solute Mobility in Articular Cartilage," J. Biomech., **30**(9), pp. 895–902.

[44] Maroudas, A., 1970, "Distribution and Diffusion of Solutes in Articular Cartilage," Biophys. J., **10**(5), pp. 365–379.

[45] Torzilli, P. A., Adams, T. C., and Mis, R. J., 1987, "Transient Solute Diffusion in Articular Cartilage," J. Biomech., **20**(2), pp. 203–214.

[46] Travascio, F., Jackson, A. R., Brown, M. D., and Gu, W. Y., 2009, "Relationship Between Solute Transport Properties and Tissue Morphology in Human Annulus Fibrosus," J. Orthop. Res., **27**(12), pp. 1625–1630.

[47] Travascio, F., and Gu, W. Y., 2007, "Anisotropic Diffusive Transport in Annulus Fibrosus: Experimental Determination of the Diffusion Tensor by FRAP Technique," Ann. Biomed. Eng., **35**(10), pp. 1739–1748.

[48] Fetter, N. L., Leddy, H. A., Guilak, F., and Nunley, J. A., 2006, "Composition and Transport Properties of Human Ankle and Knee Cartilage," J. Orthop. Res., **24**(2), pp. 211–219.

[49] Shi, C., Wright, G. J., Ex-Lubeskie, C. L., Bradshaw, A. D., and Yao, H., 2013, "Relationship Between Anisotropic Diffusion Properties and Tissue Morphology in Porcine TMJ Disc," Osteoarthritis Cartilage, **21**(4), pp. 625–633.

[50] Ngwa, W., Geier, O., Stallmach, F., Naji, L., Schiller, J., and Arnold, K., 2002, "Cation Diffusion in Cartilage Measured by Pulsed Field Gradient NMR," Eur. Biophys. J., **31**(1), pp. 73–80.

[51] Gu, W. Y., Yao, H., Vega, A. L., and Flagler, D., 2004, "Diffusivity of Ions in Agarose Gels and Intervertebral Disc: Effect of Porosity," Ann. Biomed. Eng., **32**(12), pp. 1710–1717.

[52] Kuo, J., Wright, G. J., Bach, D. E., Slate, E. H., and Yao, H., 2011, "Effect of Mechanical Loading on Electrical Conductivity in Porcine TMJ Discs," J. Dent. Res., **90**(10), pp. 1216–1220.

[53] Jackson, A. R., Yao, H., Brown, M. D., and Gu, W. Y., 2006, "Anisotropic Ion Diffusivity in Intervertebral Disc: An Electrical Conductivity Approach," Spine, **31**(24), pp. 2783–2789.

[54] Mackie, J. S., and Meares, P., 1955, "The Diffusion of Electrolytes in a Cation-Exchange Resin Membrane. 1. Theoretical," Proc. R. Soc. London, Ser. A, **232**(1191), pp. 498–509.

[55] Evans, R. C., and Quinn, T. M., 2005, "Solute Diffusivity Correlates With Mechanical Properties and Matrix Density of Compressed Articular Cartilage," Arch. Biochem. Biophys., **442**(1), pp. 1–10.
[56] Arkill, K. P., and Winlove, C. P., 2008, "Solute Transport in the Deep and Calcified Zones of Articular Cartilage," Osteoarthritis Cartilage, **16**(6), pp. 708–714.
[57] Nimer, E., Schneiderman, R., and Maroudas, A., 2003, "Diffusion and Partition of Solutes in Cartilage Under Static Load," Biophys. Chem., **106**(2), pp. 125–146.
[58] Leddy, H. A., Haider, M. A., and Guilak, F., 2006, "Diffusional Anisotropy in Collagenous Tissues: Fluorescence Imaging of Continuous Point Photobleaching," Biophys. J., **91**(1), pp. 311–316.
[59] de Visser, S. K., Crawford, R. W., and Pope, J. M., 2008, "Structural Adaptations in Compressed Articular Cartilage Measured by Diffusion Tensor Imaging," Osteoarthritis Cartilage, **16**(1), pp. 83–89.
[60] Meder, R., de Visser, S. K., Bowden, J. C., Bostrom, T., and Pope, J. M., 2006, "Diffusion Tensor Imaging of Articular Cartilage as a Measure of Tissue Microstructure," Osteoarthritis Cartilage, **14**(9), pp. 875–881.
[61] Filidoro, L., Dietrich, O., Weber, J., Rauch, E., Oerther, T., Wick, M., Reiser, M. F., and Glaser, C., 2005, "High-Resolution Diffusion Tensor Imaging of Human Patellar Cartilage: Feasibility and Preliminary Findings," Magn. Reson. Med., **53**(5), pp. 993–998.
[62] Hsu, E. W., and Setton, L. A., 1999, "Diffusion Tensor Microscopy of the Intervertebral Disc Anulus Fibrosus," Magn. Reson. Med., **41**(5), pp. 992–999.
[63] Stylianopoulos, T., Diop-Frimpong, B., Munn, L. L., and Jain, R. K., 2010, "Diffusion Anisotropy in Collagen Gels and Tumors: The Effect of Fiber Network Orientation," Biophys. J., **99**(10), pp. 3119–3128.
[64] Jackson, A. R., Travascio, F., and Gu, W. Y., 2009, "Effect of Mechanical Loading on Electrical Conductivity in Human Intervertebral Disk," ASME J. Biomech. Eng., **131**(5), p. 054505.
[65] Iatridis, J. C., and ap Gwynn, I., 2004, "Mechanisms for Mechanical Damage in the Intervertebral Disc Annulus Fibrosus," J. Biomech., **37**(8), pp. 1165–1175.
[66] ap Gwynn, I., Wade, S., Ito, K., and Richards, R. G., 2002, "Novel Aspects to the Structure of Rabbit Articular Cartilage," Eur. Cells Mater., **4**, pp. 18–29.
[67] McDevitt, C. A., and Webber, R. J., 1990, "The Ultrastructure and Biochemistry of Meniscal Cartilage," Clin. Orthop. Relat. Res., **252**, pp. 8–18.
[68] Joshi, M. D., Suh, J. K., Marui, T., and Woo, S. L., 1995, "Interspecies Variation of Compressive Biomechanical Properties of the Meniscus," J. Biomed. Mater. Res., **29**(7), pp. 823–828.
[69] Chu, C. R., Szczodry, M., and Bruno, S., 2010, "Animal Models for Cartilage Regeneration and Repair," Tissue Eng. Part B Rev., **16**(1), pp. 105–115.